Electron-impact dissociation of the methane molecule into neutral fragments

Daniel A. Erwin* and Joseph A. Kunc†
University of Southern California, Los Angeles, California 90089-1192, USA
(Received 9 August 2005; published 29 November 2005)

The three most important electron-impact processes dissociating CH_4 molecule into neutral fragments are $e+CH_4 \rightarrow CH_3+\cdots$, $e+CH_4 \rightarrow CH_2+\cdots$, and $e+CH_4 \rightarrow CH+\cdots$. Neither experimental nor theoretical cross sections for the processes in a broad range of energy are available, except for the first process for which reliable measured cross sections for energies up to 500 eV are available. Only two measured values (at a single impact energy) of the cross section for the second process are available, and only two measured values (also at a single energy) of the cross section for the third process are available in the literature. Therefore, we derive in this work analytical dissociation cross sections for the second and the third processes mentioned above in the energy range up to 500 eV. At higher (but still nonrelativistic) energies, we calculate the parameters of the Bethe-Born cross section for the second and the third processes.

DOI: 10.1103/PhysRevA.72.052719 PACS number(s): 34.10.+x, 34.50.−s, 34.50.Gb

I. INTRODUCTION

Electron-impact dissociation and ionization of the CH_4 molecule are of great interest in a variety of technological applications. Both processes are important energy sinks in nonequilibrium mixtures containing methane gas. Moreover, in plasma-assisted combustion, these processes are responsible for production of radicals such as CH which strongly affect ignition. Upon electron impact, the methane molecule can decompose into neutral fragments (CH_3, CH_2, CH, C, H_2, or H); such processes are referred to below as dissociation of the CH_4 molecule. Alternatively, the molecule can decompose into charged fragments (CH_4^+, CH_3^+, CH_2^+, CH^+, C^+, H_2^+, or H^+), processes referred to below as ionization of the CH_4 molecule.

Although theoretical studies and measurements of the probabilities of the above dissociative processes are difficult, some aspects of the processes have been studied [1–11]; the cited works show that the most important of the processes are

$$e + CH_4 \rightarrow CH_3 + \cdots , \tag{1}$$

$$e + CH_4 \rightarrow CH_2 + \cdots , \tag{2}$$

and

$$e + CH_4 \rightarrow CH + \cdots . \tag{3}$$

The existing cross sections for dissociation of the CH_4 molecule by electrons were recently critically reviewed by Shirai *et al.* [12] who recommended reliable values for only two cross sections: the cross section for the process (1) at impact energies up to 500 eV, and the total dissociation cross section (into all neutral fragments) at energies up to 1 keV. The dissociation cross section for the process (2) was not recommended in the Shirai review because of the very small amount of data for the process and significant differences between the data obtained by different authors (see the discussion below). The cross section for the process (3) is not available in the literature except for one measurement in the vicinity of the cross section maximum located at energy of about 80–100 eV [5] and one measurement at energy of 100 eV [10]. These two measurements are very valuable for testing the present theory since theoretical inelastic cross sections are typically the least accurate in the energy range close to the cross sections' maxima.

Much more reliable work has been done on electron-impact ionization of CH_4 [13–18] than on the molecular dissociation, identifying the most important ionizing processes as

$$e + CH_4 \rightarrow CH_4^+ + \cdots , \tag{4}$$

$$e + CH_4 \rightarrow CH_3^+ + \cdots , \tag{5}$$

$$e + CH_4 \rightarrow CH_2^+ + \cdots , \tag{6}$$

and

$$e + CH_4 \rightarrow CH^+ + \cdots . \tag{7}$$

The available cross sections for the electron-impact ionization of the CH_4 molecule were also reviewed in Ref. [12]. The authors recommended accurate cross sections for the processes (4) and (5) at impact energies ranging, depending on the process, from 0.5 keV to 3 keV, but no values were recommended for the processes at higher energies.

As discussed below, various comparisons of the dissociation cross sections (1)–(3) and the ionization cross sections (5)–(7) strongly indicate the presence of scaling laws relating the dissociation cross sections with each other and the ionization cross sections with each other, as well as some dissociation cross sections with some ionization cross sections. We use this fact in this work and derive the cross sections for the dissociative processes (1)–(3) in the energy range up to

*Electronic address: erwin@usc.edu
†Electronic address: kunc@usc.edu

10 keV. We do this in three stages. In the first stage, dealing with impact energies between 20–30 eV (the upper limit of the threshold law—see below) and 500 eV [the upper limit of the energy of the cross section recommended for process (1) in Ref. [12]], we exploit the scaling law relationship between the measured cross section for electron-impact dissociation of the CH_4 molecule into the neutral fragment CH_3 and the measured cross section for the electron-impact ionization of the molecule into the similar charged fragment CH_3^+. In the second stage, we derive, using the Bethe-Born approximation, the cross sections for the dissociative collisions (1) and (2) at impact energies between 500 eV and 10 keV. In the third stage we discuss the processes (1)–(3) at energies close to the dissociation thresholds E_{th}.

II. THE ROBUST SCALING LAW

The first experimental demonstration and quantitative analysis of the scaling tendencies between the total cross sections for dissociation and ionization of the CH_4 molecule by electron-impact was done by Winters [11]. He showed that the electron-impact fragmentation of the molecule into all neutral species has about the same probability as the fragmentation of the molecule into all charged species when the collision energies are smaller than those corresponding to the cross sections' maxima. Other experimental work also indicated (see below) the existence of scaling tendencies of various partial ionization and dissociation cross sections for the CH_4 molecule. These tendencies are expected because of the simple symmetry of the electronic structure of the CH_4 molecule, and because of the fact that the molecule does not have excited electronic states close to the molecular ground state.

Numerical analysis of various relationships (differences, sums, ratios, etc.) between the measured dissociation and ionization cross sections considered in this work suggests several scaling tendencies of different degrees of generality, robustness and accuracy. The analysis suggests that the most robust scaling law for the cross sections in a broad energy range is the one based on the energy dependences of some well-defined differences between the ratios of the cross sections for dissociation of the CH_4 molecule into a particular neutral fragment (e.g., CH_3) to the cross section for ionization of the molecule into a similar charged fragment (e.g., CH_3^+). In order to derive a mathematical rule for this scaling, we first define the following ratios:

$$\lambda_{mn}(E) = \frac{Q_m(E)}{Q_n(E)} \quad \text{and} \quad \lambda_{di}(E) = \frac{Q_d(E)}{Q_i(E)}, \tag{8}$$

so that

$$\lambda_{15}(E) = \frac{Q_1(E)}{Q_5(E)}, \quad \lambda_{26}(E) = \frac{Q_2(E)}{Q_6(E)}, \quad \lambda_{37}(E) = \frac{Q_3(E)}{Q_7(E)}, \tag{9}$$

where the meaning of the symbols is as follows: E is the collision impact energy, Q_m $(m=1,2,3)$ denotes the cross section for the dissociative processes (1), (2), or (3), respectively, while Q_n $(n=5,6,7)$ denotes the cross sections for the ionizing processes (5), (6), or (7), respectively. Q_d is the total cross section for the electron-impact dissociation of the CH_4 molecule into all neutral fragments, and Q_i is the total cross section for the electron-impact ionization of the molecule into all charged fragments.

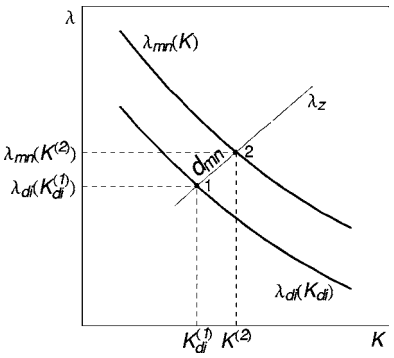

FIG. 1. The definition of the function $d_{mn}(K_{di})$ as the distance in the K-λ plane between the intersections of the curves $\lambda_{di}(K_{di})$ and $\lambda_{mn}(K)$, respectively, with the line $\lambda_z(K)$ normal to the function $\lambda_{di}(K_{di})$ at $K=K_{di}$.

The ratio $\lambda_{15}(E)$ in expression (9) can be accurately determined in a broad range of energy (up to 500 eV) from the experimental data of Ref. [12], but the ratios $\lambda_{26}(E)$ and $\lambda_{37}(E)$ cannot be obtained since accurate cross sections $Q_2(E)$ and $Q_3(E)$ are not available in the energy range important in typical studies of the dissociation of the CH_4 molecule. It is, therefore, one of the goals of this work to find a scaling law that would lead to acceptable ratios λ_{26} and λ_{37} and, subsequently, to the cross sections Q_2 and Q_3, in a broad range of energy.

We introduce a convenient new variable, the dimensionless impact energy K, defined as

$$K = E/I_5, \quad \text{so that } K_{di} = E_{di}/I_5, \tag{10}$$

where K_{di} and K, respectively, are the energies of the intersection points 1 and 2 in Fig. 1, and $I_5=14.24$ eV is the ionization threshold for the process (5). The choice of the energy I_5 is of course arbitrary, but we choose this energy as the threshold for the e-CH_4 inelastic process to emphasize the fact that it should be possible in the future to establish a direct and explicit dependence of the scaling laws for the ionization and dissociation cross sections on the energy thresholds of the processes.

The scaling law discovered in our numerical analysis of various relationships of the measured dissociation and ionization cross sections of Ref. [12] is based on the observation that the distance $d_{mn}(K_{di})$ in the K-λ plane (see Fig. 1) between the ratio $\lambda_{mn}(K)$ and the ratio $\lambda_{di}(K_{di})$ for $mn \equiv 26$ and $mn \equiv 37$ differs at energies between 20 eV and 500 eV by a constant factor α_{mn} from the distance d_{15} [see relationship (14)]. At energy K_{di}, $d_{mn}(K_{di})$ is defined as the distance along the line $\lambda_z(K)$ between the curves $\lambda_{di}(K)$ and $\lambda_{mn}(K)$. The line $\lambda_z(K)$ is normal to the curve $\lambda_{di}(K)$ at the point K_{di}, $\lambda_{di}(K_{di})$. The equation of the normal is

$$\lambda_z(K) = -(\partial\lambda_{di}/\partial K)^{-1}_{K=K_{di}}(K-K_{di}) + \lambda_{di}(K_{di}). \tag{11}$$

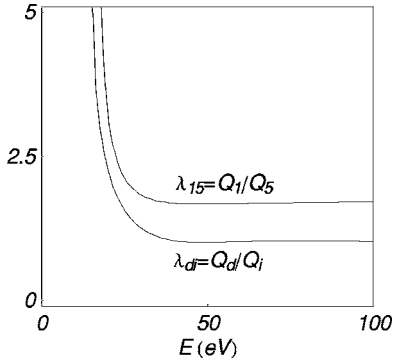

FIG. 2. The ratios Q_1/Q_5 and Q_d/Q_i obtained from the measured cross sections Q_1, Q_5, Q_d, and Q_i recommended in the review of Shirai *et al.* [12].

Numerical solution of the equations

$$\lambda_z(K_{di}) = \lambda_{di}(K_{di}) \quad \text{and } \lambda_z(K) = \lambda_{mn}(K), \tag{12}$$

for a particular value of K_{di} yields coordinates of the intersections of the curves $\lambda_{di}(K_{di})$ and $\lambda_{mn}(K)$ with the line $\lambda_z(K)$, and thus determines the function $d_{mn}(K_{di})$,

$$d_{mn}(K_{di}) = \{[\lambda_{mn}(K) - \lambda_{di}(K_{di})]^2 + (K - K_{di})^2\}^{1/2}. \tag{13}$$

The relationship (13) for $mn \equiv 15$ is shown in Fig. 2. As can be seen, the dependence of d_{15} on the energy is weak at energies between 20 eV and 100 eV, and this is true also for energies between 100 eV and 500 eV (the upper limit of energy for which the cross section Q_1 is available in Ref. [12]). The robustness of this tendency can be seen in Figs. 3 and 4 where the ratio Q_d/Q_i is both qualitatively and quantitatively very different from the ratio Q_1/Q_5, yet the function d_{15} shows weak dependence on the impact energy in the entire energy range considered.

Taking the above into account, we assume in what follows that in the energy range between 20 eV and 500 eV the unknown functions $d_{26}(K_{di})$ and $d_{37}(K_{di})$ scale with respect to the known function $d_{15}(K_{di})$ as ($mn \equiv 26$ or 37),

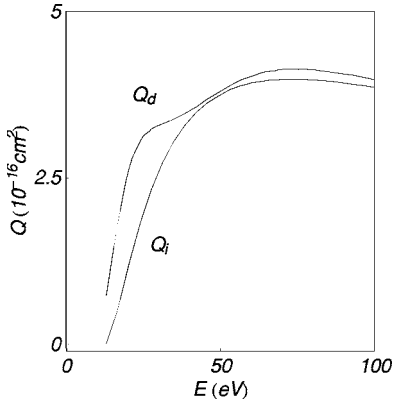

FIG. 3. The measured total cross sections recommended in the review of Shirai *et al.* [12] for dissociation (Q_d) and ionization (Q_i) of the CH_4 molecule by electron impact.

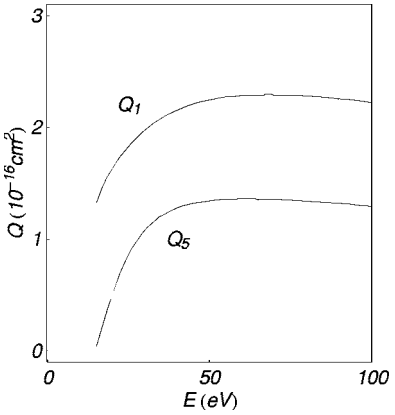

FIG. 4. The measured cross sections recommended in the review of Shirai *et al.* [12] for the cross sections Q_1 and Q_5 for the processes (1) and (5), respectively.

$$d_{mn}(K_{di}) = \alpha_{mn} d_{15}(K_{di}), \tag{14}$$

where the constant scaling factor α_{mn} is discussed below, and the energy dependence of d_{15} is shown in Fig. 5. Subsequently, the ratios $\lambda_{26}(K_{di})$ and $\lambda_{37}(K_{di})$ can be obtained from Eq. (13) as

$$\lambda_{mn}(K) = \lambda_{di}(K_{di}) + [d_{mn}^2(K_{di}) - (K - K_{di})^2]^{1/2}. \tag{15}$$

Numerical analysis shows that even at energies between 20 eV and 500 eV, the second term in the curly braces in relationship (15) can be neglected when compared to the first term in the braces. This allows one to assume that $K_{di} = K$. Thus, the values of the ratios $\lambda_{26} = Q_2/Q_6$ and $\lambda_{37} = Q_3/Q_7$ at a given energy K can be given by

$$\lambda_{mn}(K) = \lambda_{di}(K) + d_{mn}(K) \simeq \lambda_{di}(K) + \alpha_{mn} d_{15}(K), \tag{16}$$

and the unknown cross sections $Q_2(E)$ and $Q_3(E)$ at energies between 20 eV and 500 eV can be obtained from (with $m = 2$ and 3, respectively),

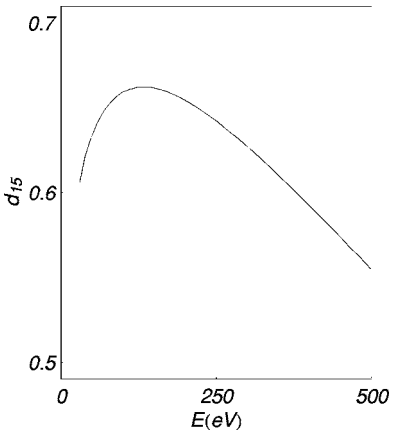

FIG. 5. The function d_{15} obtained from the relationship (23).

$$Q_m(E) = Q_n(E)\left[\frac{Q_d(E)}{Q_i(E)} + \alpha_{mn} d_{15}(E)\right], \tag{17}$$

where all the cross sections on the right-hand-side are those recommended in Ref. [12], and the function $d_{15}(E)$ is obtained from expression (13) also using the cross sections Q_1 and Q_5 recommended there. For practical purposes, we fit the cross sections by the following expressions of accuracy better than one percent for $E > 20$ eV (the cross sections are in 10^{-16} cm^2 when E is in eV):

$$Q_d(E) = \frac{4.48 \times 10^7 (E')^{3.590} + 19.83 (E')^{7.525}}{1.14 \times 10^{11} + 4.46 \times 10^6 (E')^{3.935} + (E')^{7.870}}, \tag{18}$$

where $E' \equiv E - 4.51$ eV,

$$Q_i(E) = \frac{10.26 \ln E - 25.94}{E[3.77 \times 10^{-2} + (E-13)^{-0.906}]}, \tag{19}$$

$$Q_5(E) = \frac{5.55 \times 10^{-2} (E')^{1.435}}{1 + 0.0257 (E')^{1.509} + 2.59 \times 10^{-5} (E')^{2.635}}, \tag{20}$$

where $E' \equiv E - 14.24$ eV,

$$Q_6(E) = \frac{9.22 (E')^{1.868}}{10^4 + 4.66 (E')^{2.168} + 0.10 (E')^{2.868}}, \tag{21}$$

where $E' \equiv E - 15.20$ eV,

$$Q_7(E) = \frac{5.01 \times 10^{-3} (E')^{1.161}}{1 + 0.001\,17 (E')^{1.831} + 1.19 \times 10^{-6} (E')^{2.761}}, \tag{22}$$

where $E' \equiv E - 24.14$ eV, and

$$d_{15}(E) = 0.4084 e^{-0.00093} E^{0.1241}. \tag{23}$$

The scaling factor $\alpha_{15} = 1$ and the scaling factors α_{26} and α_{37} can be obtained if at least single values of the cross sections Q_2 and Q_3 are available for some energy between 20 eV and 500 eV. Fortunately, two experimental values of each of the cross sections Q_2 and Q_3 are available close to the cross sections' maxima where the theoretical cross sections are the least accurate. The values are those measured at $E = 100$ eV by Melton and Rudolf [10] ($Q_2^M = 0.2 \times 10^{-16}$ cm^2 and $Q_3^M = 0.1 \times 10^{-16}$ cm^2), and those measured at $E = 75$ eV by Tahara *et al.* [5] ($Q_2^T = 0.62 \times 10^{-16}$ cm^2 and $Q_3^T = 0.31 \times 10^{-16}$ cm^2). As can be seen in Table I, the dissociation cross section $Q_1^M = 1.2 \times 10^{-16}$ cm^2 measured by Melton and Rudolf at $E = 100$ eV is 0.54 of the corresponding reliable dissociation cross section of Shirai *et al.*, $Q_1^S = 2.22 \times 10^{-16}$ cm^2. Expecting that the relative systematic errors of Melton and Rudolf's measurements of the cross sections Q_2 and Q_3 are similar to the errors of their measurements of the cross section Q_1, the more realistic values of Q_2^M and Q_3^M in the Melton and Rudolf experiment should be 0.38×10^{-16} cm^2 and 0.18×10^{-16} cm^2, respectively.

The cross section measured by Tahara *et al.* for the process (1), $Q_1^T = 3.74 \times 10^{-16}$ cm^2 at $E = 75$ eV, is 1.63 times greater than the corresponding cross section recommended by Shirai *et al.* Assuming again that the relative systematic errors of the measurements of Tahara *et al.* of the cross sections Q_2 and Q_3 are similar to the errors of their measurements of the cross section Q_1, the more realistic values of their measurements should be 0.37×10^{-16} cm^2 (Q_2^T) and 0.18×10^{-16} cm^2 (Q_3^T), values very close to values of Q_2^M and Q_3^M obtained in the preceding paragraph. The realistic cross sections measured by Melton and Rudolf and by Tahara *et al.* would not change more than 10% in the energy interval between 75 eV and 100 eV since the maxima of the cross sections are located in this interval. Therefore, we use in our calculations of the scaling factors α_{26} and α_{37} the cross sections $Q_2(E = E^0) = 0.37 \times 10^{-16}$ cm^2 and $Q_3(E = E^0) = 0.18 \times 10^{-16}$ cm^2 ($E^0 = 100$ eV) (see the column "pw" in Table I).

TABLE I. Available measured cross sections (in 10^{-16} cm^2) for dissociation and ionization of the CH_4 molecule by electrons of energy $E \simeq 100$ eV, except for the three cross sections shown in the fifth column which were measured at energies of 75 eV. The last column marked "pw" shows the cross sections used in the present work to calculate the scaling factors α_{26} and α_{37}.

Q	Ref. [12]	Ref. [10]	Ref. [16]	Ref. [5]	pw
Q_d	3.98	4.70			3.98
Q_i	3.86	3.80	3.55		3.86
Q_1	2.22	1.20		3.74	2.22
Q_2		0.20		0.62	0.37
Q_3		0.10		0.31	0.18
Q_4	1.57	1.80	1.78		1.57
Q_5	1.29	1.50	1.35		1.29
Q_6	0.32	0.28	0.23		0.32
Q_7	0.17	0.14	0.10		0.17

Taking the above into account, the scaling factors $\alpha_{26}(E)$ and $\alpha_{37}(E)$ can be given as ($mn = 26$ and 37, respectively)

$$\alpha_{mn} = \frac{d_{mn}^0}{d_{15}} = \frac{[(Q_m^0)/(Q_n^0)] - [(Q_d^0)/(Q_i^0)]}{d_{15}^0}, \tag{24}$$

where the superscript 0 denotes the value at $E = E^0$, and $d_{15}^0 = 0.659$. The values of the required cross sections are given in column "pw" of Table I. Thus,

$$\alpha_{26} = 0.190 \quad \text{and} \quad \alpha_{37} = 0.042. \tag{25}$$

III. DISSOCIATION OF CH_4 INTO THE CH_2 OR CH FRAGMENTS

A. Collisions at energies 20 eV $\leqslant E \leqslant$ 500 eV

The cross sections Q_2 and Q_3 obtained from the relationships (17)–(25) are shown in Fig. 6 together with several relevant measurements available in the literature. The figure also compares the cross section Q_1 of the present work with that recommended in Ref. [12] to validate the approach used in this work.

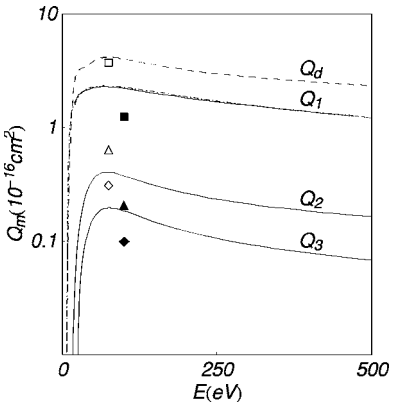

FIG. 6. The cross sections Q_1, Q_2, and Q_3 of the present work (solid lines) for the processes (1)–(3), respectively. The dashed curve and the dotted-dashed curve are the experimental cross section Q_1 and Q_2, respectively, recommended in Ref. [12]. The open symbols are the measured cross sections of Tahara *et al.* [5] and the filled symbols the cross sections of Melton and Rudolf [10]. In both cases, the squares, triangles, and diamonds represent the cross sections Q_1, Q_2, and Q_3, respectively.

B. Collisions at energies 0.5 keV $< E \leqslant$ 10 keV

At high, but nonrelativistic, impact energies, ionization and dissociation of CH_4 molecules by electrons can be accurately described by the Bethe-Born approximation [19] which yields the following cross sections for the dissociation processes (1)–(3) ($m \equiv 1$, 2, and 3, respectively),

$$Q_m(E) = A_m E^{-1} \ln B_m E, \tag{26}$$

where $Q_m(E)$ is in cm^2 if the collision impact energy E is in eV, and the constants A_m and B_m have the values given below.

We calculate the cross sections for the processes (1)–(3) at nonrelativistic energies greater than 500 eV using the Bethe-Born approximation and the values of the cross sections at energies somewhat smaller (within 25 eV) than 500 eV. [Thus, we assume here that the Bethe-Born approximation also applies to collisions (1)–(3) at impact energies between 475 eV and 500 eV, which is usually well justified in dissociation of molecules by electrons at such energies.] As a result one obtains

$$A_1 = 262.68 \times 10^{-16}\ \text{cm}^2\ \text{eV},$$

$$A_2 = 39.84 \times 10^{-16}\ \text{cm}^2\ \text{eV},$$

$$A_3 = 12.27 \times 10^{-16}\ \text{cm}^2\ \text{eV}, \tag{27}$$

and

$$B_1 = 0.020\ \text{eV}^{-1}, \quad B_2 = 0.015\ \text{eV}^{-1}, \quad B_3 = 0.031\ \text{eV}^{-1}. \tag{28}$$

C. The threshold laws

The dissociation energies for the processes (2) and (3) are not accurately known, and the realistic energy dependences of the cross sections Q_1, Q_2, and Q_3 close to their thresholds (that is, at energies between the thresholds and about 20 eV) are not available. Since the fitting formulas of Shirai *et al.* [12] for the cross sections were derived from the measured cross sections which are reliable for energies above 20 eV, the formulas should not be used as highly accurate approximations of the threshold laws for the processes.

There have been a few attempts to study in detail the threshold laws of the cross sections Q_1, Q_2, and Q_d, with the threshold law of the latter cross section being the first to be studied experimentally [11]. That study concluded that the near-threshold energy dependence of Q_d is a linear function with the dissociation energy being equal to about 10 eV. This set up a long-lasting standard used in almost all studies of the subject. The studies have consistently assumed linear threshold laws not only for the cross section Q_d but also for the cross sections Q_1, Q_2, and Q_3 despite the lack of theoretical basis for the linearity [20], and the single energy value of 10 eV was also often assumed in the early studies for the dissociation energies of processes (1)–(3).

The threshold laws for collisions such as (1), (2), and (3) cannot be linear [20] and the dissociation energies of the processes must differ markedly from one another. This has been confirmed recently [12] by establishing the dissociation energy of the process (1) as being not 10 eV but rather 4.51 eV.

The most detailed experimental attempts to establish the near-threshold dependence of the cross sections Q_1 and Q_2 are discussed in Refs. [2] and [7]; see also Ref. [21]. However, the low resolution of the results and the fact that the authors did not establish accurate values of the process thresholds prevents reliable conclusions about the processes' threshold laws. Thus, one can say that it is necessary to have more high-resolution work done on the collisions (1)–(3) at energies close to their thresholds before some acceptable threshold laws for the processes can be proposed.

IV. FINAL REMARKS

The main results of this work are the cross sections Q_1, Q_2, and Q_3 shown in Fig. 6. The excellent agreement of the present cross section Q_1 with the experimental data of Ref. [12] in the entire considered energy range is a reliable validation of the theoretical approach of the present work. One should notice that the close-to-maximum cross sections of the present work are consistently between the measured results of Tahara *et al.* [5] and those of Melton and Rudolf [10]. As discussed above, it seems that at impact energies between 75 eV and 100 eV the cross sections measured by Tahara *et al.* are too high, while the cross sections measured by Melton and Rudolf are too small. Thus, the results shown in Fig. 6 and Table I strongly suggest that the cross sections Q_2 and Q_3 of the present work should also be satisfactory representations of the dissociative dynamics of the collisions (1)–(3) at energies between 20 eV and 500 eV. The same can be said about the validity of the present results at high energies (0.5–10 keV) since the Bethe-Born approximation used here to obtain these high-energy cross sections has been ex-

ceptionally successful in predicting the high-energy cross sections for electron-impact ionization and dissociation of atoms and molecules.

It should be emphasized that the accuracy of the present approach depends on the accuracies of the experimental cross sections recommended in Ref. [12] and used in our calculations. Since the recommended cross sections seem to be quite accurate representations of reality, the cross sections Q_1, Q_2, and Q_3 of this work should be acceptable in most applications. No recommendations are made in the present work for theoretical treatment of the collisions at energies less than about 20 eV, the region of the threshold law.

[1] W. Y. Fan, P. F. Knewstubb, M. Koning, L. Mechold, J. Ropcke, and P. B. Davies, J. Phys. Chem. A **103**, 4118 (1999).
[2] S. Motlagh and J. H. Moore, J. Chem. Phys. **109**, 432 (1998).
[3] G. Garcia and F. Manero, Phys. Rev. A **57**, 1069 (1998).
[4] K. Motohashi, H. Soshi, M. Ukai, and S. Tsurubuchi, Chem. Phys. **213**, 369 (1996).
[5] H. Tahara, K. Minami, A. Murai, T. Yasui, and T. Yoshikawa, Jpn. J. Appl. Phys., Part 1 **34**, 1972 (1995).
[6] P. Bou, J. C. Boettner, and L. Vandenbulcke, Jpn. J. Appl. Phys., Part 1 **31**, 1505 (1992).
[7] T. Nakano, H. Toyoda, and H. Sugai, Jpn. J. Appl. Phys., Part 1 **30**, 2912 (1991).
[8] D. K. Davis, L. E. Kline, and W. E. Bies, J. Appl. Phys. **65**, 3311 (1989).
[9] K. Tachibana, M. Nishida, H. Harima, and Y. Urano, J. Phys. D **17**, 1727 (1984).
[10] C. E. Melton and P. S. Rudolf, J. Chem. Phys. **47**, 1771 (1967).
[11] H. F. Winters, J. Chem. Phys. **63**, 3462 (1975).
[12] T. Shirai, T. Tabata, H. Tawara, and Y. Itikawa, At. Data Nucl. Data Tables **80**, 147 (2002).
[13] H. C. Straub, D. Lin, B. G. Lindsay, K. A. Smith, and R. F. Stebbings, J. Chem. Phys. **106**, 4430 (1997).
[14] H. C. Straub, P. Renault, B. G. Lindsay, K. A. Smith, and R. F. Stebbings, Phys. Rev. A **54**, 2146 (1996).
[15] O. J. Orient and S. K. Srivastava, J. Phys. B **20**, 3923 (1987).
[16] H. Chatham, D. Hils, R. Robertson, and A. Gallagher, J. Chem. Phys. **81**, 1770 (1984).
[17] B. Adamczyk, A. J. Boerboom, B. L. Schram, and J. Kistemaker, Chem. Phys. **44**, 4640 (1966).
[18] D. Rapp and P. J. Englander-Golden, J. Chem. Phys. **43**, 1464 (1965).
[19] N. F. Mott and H. S. W. Massey, *Theory of Atomic Collisions* (Clarendon, New York, 1969).
[20] G. H. Wannier, Phys. Rev. **100**, 1180 (1955).
[21] C. Winstead, Q. Sun, V. McKoy, L. L. da Silva Lino, and M. A. Lima, Z. Phys. D: At., Mol. Clusters **24**, 141 (1992).